Spherical indentation analysis of stress relaxation for thin film viscoelastic materials

Spherical indentation analysis of stress relaxation for thin film viscoelastic materials

D Cheneler[a,*], N Mehrban[b], J Bowen[b]
[a] *School of Mechanical Engineering, University of Birmingham, Birmingham, UK*
[b] *School of Chemical Engineering, University of Birmingham, Birmingham, UK*

* Corresponding author. Tel.: +44 121 414 4256; fax: +44 121 414 3958.
E-mail address: D.Cheneler@bham.ac.uk

Abstract
The mechanical testing of thin layers of soft materials is an important but difficult task. Spherical indentation provides a convenient method to ascertain material properties whilst minimising damage to the material by allowing testing to take place in situ. However, measurement of the viscoelastic properties of these soft materials is hindered by the absence of a convenient yet accurate model which takes into account the thickness of the material and the effects of the underlying substrate. To this end, the spherical indentation of a thin layer of viscoelastic solid material is analysed. It is assumed that the transient mechanical properties of the material can be described by the generalised standard linear solid model. This model is incorporated into the theory and then solved for the special case of a stress relaxation experiment taking into account the finite ramp time experienced in real experiments. An expression for the force as a function of the viscoelastic properties, layer thickness and indentation depth is given. The theory is then fitted to experimental data for the spherical indentation of poly(dimethyl)siloxane mixed with its curing agent to the ratios of 5:1, 10:1 and 20:1 in order to ascertain its transient shear moduli and relaxation time constants. It is shown that the theory correctly accounts for the effect of the underlying substrate and allows for the accurate measurement of the viscoelastic properties of thin layers of soft materials.

Keywords
Transient shear moduli; Generalised standard linear solid model; Stress relaxation; Spherical indentation; Soft solids

Introduction

The determination of material properties of thin layers of soft solids is an important process in a number of areas such as polymer and biomaterials engineering where the surface orientation, strength and structure of scaffolds in tissue engineering determine good/bad cellular attachment (Levental et al. 2010). Typical materials that need to be tested include polymeric tribological coatings (Jardet and Morel 2003) and even living cells (Wakatsuki 2001).

Viscoelastic properties can be obtained for bulk materials by performing conventional creep or relaxation tests in standardised experiments, such as the uniaxial tension test. However, it is impossible to conduct these tests when the sample size is small like in the case of thin films. Also, soft solids can be inherently difficult to handle. Fortunately, indentation provides a reliable technique for ascertaining the properties of these materials without damaging them. Hence, indentation is increasingly being used for determining the viscoelastic properties of materials (Darling et al. 2006; Moreno-Flores et al. 2010) and has been extensively used to measure properties such as Young's modulus and hardness of materials that show time independent behaviour (Zhang et al. 2004). However, the disadvantage to this method is that during experimentation, only the displacement of the indenter and the force acting upon it are known. In order to ascertain material properties, it is necessary to have deduced the stress field within the material.

Typically, the Hertzian model of a sphere indenting an elastic half space has been assumed (Hertz 1882). This model has been subsequently developed to include viscoelasticity of the material using the superposition principle (Ting 1966; Greenwood 2010; Lee and Radok 1960) and has been successfully employed in the analysis of biological materials (Darling et al. 2006; Moreno-Flores et al. 2010). The Hertz model is only applicable within certain limits. Hertzian theory assumes that the bodies in contact are smooth, isotropic, homogenous and linearly elastic (Dintwa et al. 2008). For spherical indentation into a flat surface, as is of interest here, the indentation depth, δ has to be kept sufficiently small so that the radius of the contact area, a, given by $a^2 = R\delta$ is less than 10% of the sphere radius, R, so that the quadratic approximation for the shape of the sphere is accurate (Landau and Lifshitz 1986).

Complications arise with this particular model when the material is sufficiently thin so that the indention is affected by the underlying substrate, which is generally assumed to be of a much higher modulus than the material. In these cases the calculated moduli are too high, sometimes by orders of magnitude, and the material appears to be stiffer than expected (Domke and Radmacher 1998). Historically, analytical expressions using integral transforms were derived to find the stress and displacement fields (Bufler 1971; Fretigny and Chateauminois 2000; Chen 1971). However, these methods still generally require sophisticated mathematical manipulations or extensive numerical computations (Tu and Gazis 1964; Dhaliwal and Rau 1970; Chen and Engel 1972). The inconvenience of using these solutions has largely precluded their use by experimentalists who need a simple solution to compare experiments to. Dimitriadis *et al.* (Dimitraidais et al. 2002), following on from Chadwick's earlier work (Chadwick 2002), derived simpler analytical corrections to the Hertzian model. Experiments analysed using the correction by Dimitriadis *et al.* (Dimitraidais et al. 2002) showed that the elastic modulus remained consistent with the macroscopic experiments regardless of film thickness and indentation depth

This paper concentrates on the extension of the work of Dimitriadis *et al.* (2002) to viscoelastic materials. Previous researchers have attempted this by appending the correction terms afore mentioned onto the viscoelastic version of the Hertzian model (Darling et al. 2007). However, the correction given by Dimitriadis *et al.* (2002) is due to a superposition of stress states, each of which have a transient response due to the change in the contact radius in time (Greenwood 2010). The change in each stress state needs to be taken into account, as does the loading time of the indenter in order to correctly describe the mechanics of the indentation experiment. To this end, a general equation describing the indentation of a viscoelastic thin solid film is derived. So that the theory can be used to describe as many soft solids as possible, it is assumed that the viscoelastic response of the material can be described by the generalised standard linear model (Ferry 1980). This model is used in the theory and then solved for the specific case of a stress relaxation experiment by employing the correspondence principle, the validity of which is discussed. It is shown that by using this theory, the viscoelastic moduli, specifically the relaxation moduli, can be found directly. Furthermore it is shown that these moduli, as calculated from experimental data, are not a function of the film thickness or penetration depth, as they would be if calculated using Hertzian models without the thin film correction. The theory therefore constitutes a good foundation for the determination of viscoelastic properties of soft solids using indentation.

Theory

Transient Indentation of a Viscoelastic Half-Space

The indentation of a viscoelastic half-space by a sphere can be modelled by assuming Hertzian contact. This is achieved by first considering the material to be elastic in order to ascertain the pressure distribution in the material due to the indentation of the sphere, then by employing the correspondence principle to incorporate the viscoelasticity of the material. If the modulus of the material is much smaller than the moduli of the sphere, which is usually the case with polymer and biological material, the sphere is then considered to be a rigid body. The contact between the sphere and material surface is assumed to be frictionless. In this case, with contact occurring between a rigid sphere and a soft flat material, the effective reduced elastic modulus is defined as (Johnson 1985):

$$E^* = \frac{E}{1-\nu^2} \qquad (1)$$

where E and ν is the materials Young's modulus and Poisson's ratio respectively. For contact of this nature, Hertz proved the pressure distribution is of the form (Johnson 1985):

$$p(r) = \frac{2E^*\delta}{\pi a}\left(1-\frac{r^2}{a^2}\right)^{1/2} \qquad (2)$$

where r is the radial distance from the centre of the sphere (see Fig. 1). The force exerted by the sphere onto the material can therefore be given as:

$$F_0 = \int_0^a 2\pi r p(r)\mathrm{d}r = \frac{4}{3R}a^3E^* \qquad (3)$$

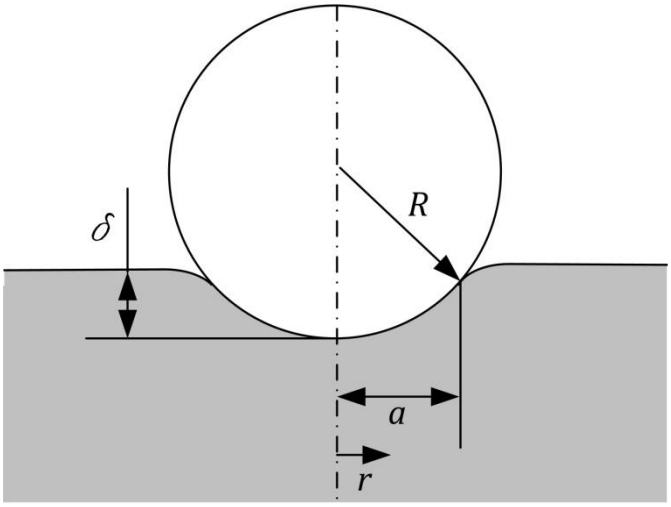

Fig. 1: The geometry used in Hertzian contact analysis.

As the sphere is assumed to be rigid and the material can be described as incompressible with a shear modulus G, the expression for the indentation force for an incompressible elastic half-space can be written as (Lee and Radok 1960):

$$F_0 = \frac{8}{3R}(2G)a^3 \qquad (4)$$

When the material is viscoelastic and δ and F_0 vary with time, the $2G$ in eq. 4 becomes transient and is therefore replaced by the relaxation operator for the material, $\Psi(t)$. This is known as the correspondence principle. Not all problems can be solved using the correspondence principle. Such problems include those whereby the type of boundary condition on a surface changes with time. For instance if the boundary condition changes from traction to displacement controlled, the problem cannot be solved using the correspondence principle. However, the conditions themselves can be time dependent (Rizzo and Shippy 1971; Findlay et al. 1976). The readers are encouraged to read more thorough explanations of the correspondence principle by Johnson and by Lee and Radok (Johnson 1985; Lee and Radok 1960). As spherical indentation results in a change in the contact radius, in general the correspondence principle is invalid. However there is a variation of the principle that remains valid for bodies occupying fixed regions in space, even if the type of boundary condition changes with time (Graham and Sabin 1973). This variation is valid only in the cases where the contact area is monotonically increasing with time (Cao et al. 2009). It is for this reason why the experiment to be described is a stress relaxation experiment. In this case the position of the sphere, and in turn the contact radius, is controlled and it is ensured that the contact radius is either monotonically increased or kept constant. Thus the contact force is given by:

$$F_0(t) = \frac{8}{3R}\int_0^t \Psi(t-t')\frac{\mathrm{d}}{\mathrm{d}t'}a^3(t')\mathrm{d}t' \qquad (5)$$

The relaxation operator depends on the model chosen to best describe the viscoelastic behaviour of the material. In this paper a generalised standard linear model has been chosen as the basis for the relaxation operator which has been derived in the appendix to give:

$$\Psi(t) = 2G_\infty + 2\sum_{n=1}^{N} G_n e^{-t/T_n} \qquad (6)$$

For stress relaxation, the experiment is displacement controlled therefore the penetration depth can be defined as:

$$\delta(t) = v_d t - v_d(t-t_{dr})H(t-t_{dr}) \qquad (7)$$

where v_d is the velocity of the sphere downwards, t is the time, t_{dr} is the time of the downwards ramp, H is the Heaviside function. This function describes the motion of the sphere which is moved downwards at a constant velocity to a specific depth defined by $\delta_0 = v_d t_{dr}$ and held for a period of time as shown in Fig. 2. This in turn

defines the contact radius. As the contact radius is monotonically increasing, there is no need to consider unloading effects (Ting 1966; Greenwood 2010). The form of eq. 7 is in contrast to the majority of indentation studies where step-loading conditions have been assumed which is analytically convenient but experimentally impossible to implement (Zhang et al. 2004).

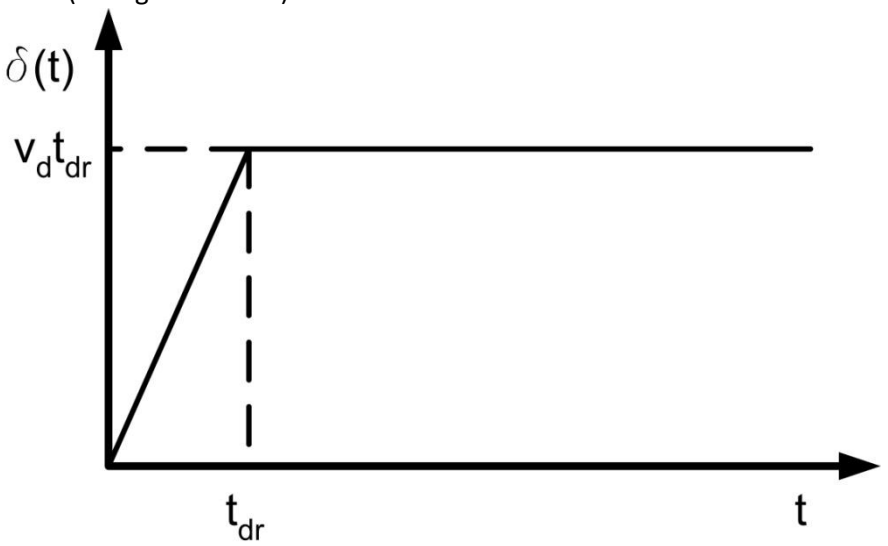

Fig. 2: Schematic of the displacement of the sphere during a stress relaxation experiment as described by eq. 7.

Given eq. 7, when $t < t_{dr}$ $a^3 = R^{3/2} V_d^{\,3/2} t^{3/2}$ therefore $da^3/dt' = (3/2) R^{3/2} V_d^{\,3/2} t'^{1/2}$ else $da^3/dt' = 0$. Upon substituting these terms and eq. 6 into eq. 5, the viscoelastic solid equivalent to eq. 4 for the stress relaxation experiment can be seen to be:

$$F_0(t) = \begin{cases} 8R^{1/2} V_d^{\,3/2} \int_0^t \left[G_\infty + \sum_{n=1}^{N} G_n e^{-(t-t')/T_n} \right] t'^{1/2}\, \mathrm{d}t' & if \quad t < t_{dr} \\ 8R^{1/2} V_d^{\,3/2} \int_0^{t_{dr}} \left[G_\infty + \sum_{n=1}^{N} G_n e^{-(t-t')/T_n} \right] t'^{1/2}\, \mathrm{d}t' & otherwise \end{cases} \tag{8}$$

And upon solving:

$$F_0(t) = \begin{cases} \frac{16}{3R} G_\infty \left(R v_d t \right)^{\frac{3}{2}} + 8R^{\frac{1}{2}} v_d^{\frac{3}{2}} \sum_{n=1}^{N} \left\{ G_n T_n^{\frac{3}{2}} \left[\sqrt{\frac{t}{T_n}} - D\left(\sqrt{\frac{t}{T_n}} \right) \right] \right\} & if \quad t < t_{dr} \\ \frac{16}{3R} G_\infty \left(R v_d t_{dr} \right)^{\frac{3}{2}} + 8R^{\frac{1}{2}} v_d^{\frac{3}{2}} \sum_{n=1}^{N} \left\{ G_n T_n^{\frac{3}{2}} e^{-\frac{(t-t_{dr})}{T_n}} \left[\sqrt{\frac{t_{dr}}{T_n}} - D\left(\sqrt{\frac{t_{dr}}{T_n}} \right) \right] \right\} & otherwise \end{cases} \tag{9}$$

where $D(x)$ is the Dawson's integral defined as:

$$D(x) = e^{-x^2} \int_0^x e^{t^2} dt \tag{10}$$

Thin Film Correction

Dimitradis *et al.* (2002) derived a correction to eq. 3 to take into account the effects of the material having a finite thickness. The expression was given to fourth order as:

$$F = \frac{4E}{3(1-\nu^2)} R^{1/2} \delta^{3/2} \left[1 - \frac{2\alpha_0}{\pi} \chi + \frac{4\alpha_0^2}{\pi^2} \chi^2 - \frac{8}{\pi^3} \left(\alpha_0^3 + \frac{4\pi^2}{15} \beta_0 \right) \chi^3 + \frac{16\alpha_0}{\pi^4} \left(\alpha_0^3 + \frac{3\pi^2}{5} \beta_0 \right) \chi^4 \right] \tag{11}$$

where $\chi = \sqrt{R\delta} / h$, h being the film thickness (see Fig. 3) and the constants α_0 and β_0 are functions of the Poisson's ratio of the film.

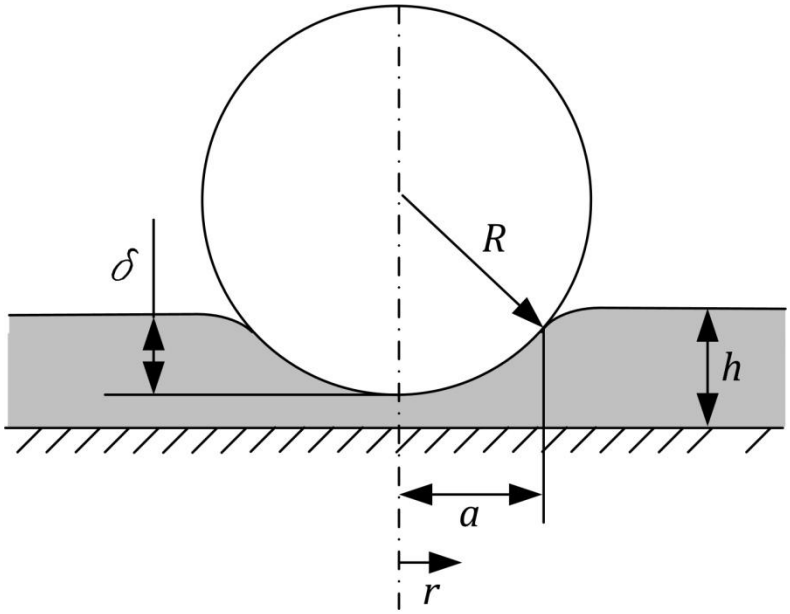

Fig. 3: The geometry used in thin film contact analysis. Note the deformation of the film surface when $r > a$ is dependent on the Poisson's ratio of the material and the shape shown here is purely representative.

For the case where the film is bonded to the underlying substrate they are given by (Dimitraidais et al. 2002):

$$\alpha_0 = -\frac{1.2876 - 1.4678\nu + 1.3442\nu^2}{1-\nu},$$
$$\beta_0 = \frac{0.6387 - 1.0277\nu + 1.5164\nu^2}{1-\nu} \quad (12)$$

When it is not bonded to the underlying substrate, the constants are given by (Dimitraidais et al. 2002):

$$\alpha_0 = -0.347\frac{3-2\nu}{1-\nu},$$
$$\beta_0 = 0.056\frac{5-2\nu}{1-\nu} \quad (13)$$

In order to make the thin film correction, eq. 11, viscoelastic, the same procedure needs to be followed. To do this it needs to be recognised that eq. 11 can be presented in the form:

$$F = \frac{4E^*}{3R}(R\delta)^{3/2}\left[1 + C_1\chi + C_2\chi^2 + C_3\chi^3 + C_4\chi^4\right] \quad (14)$$

where the constants $C_1 ... C_4$ can be found by comparing eq. 14 to eq. 11. In terms of the contact radius eq. 14 can be presented as:

$$F = \frac{4E^*}{3R}a^3 + C_1\frac{4E^*}{3Rh}a^4 + C_2\frac{4E^*}{3Rh^2}a^5 + C_3\frac{4E^*}{3Rh^3}a^6 + C_4\frac{4E^*}{3Rh^4}a^7 \quad (15)$$

Using the correspondence principle as before it can be seen that the higher order corrections in the viscoelastic case can be given as:

$$F_1(t) = \frac{8C_1}{3Rh}\int_0^t \Psi(t-t')\frac{\mathrm{d}}{\mathrm{d}t'}a^4(t')\mathrm{d}t' \quad (16)$$

$$F_2(t) = \frac{8C_2}{3Rh^2}\int_0^t \Psi(t-t')\frac{\mathrm{d}}{\mathrm{d}t'}a^5(t')\mathrm{d}t' \quad (17)$$

$$F_3(t) = \frac{8C_3}{3Rh^3}\int_0^t \Psi(t-t')\frac{\mathrm{d}}{\mathrm{d}t'}a^6(t')\mathrm{d}t' \quad (18)$$

$$F_4(t)=\frac{8C_4}{3Rh^4}\int_0^t \Psi\left(t-t'\right)\frac{\mathrm{d}}{\mathrm{d}t'}a^7(t')\mathrm{d}t' \tag{19}$$

Where the total force is given as:

$$F(t)=F_0(t)+F_1(t)+F_2(t)+F_3(t)+F_4(t) \tag{20}$$

The first term is given by eq. 9 while the other terms are corrections. Eq. 22 could in principle be solved numerically. However, if the properties of the material were desired and the numerical solution would need to be incorporated into a curve fitting algorithm, this method would be very computationally expensive. Fortunately for the case of the stress relaxation experiment described above, there is an analytical solution, which can be shown to be:

$$F_1(t)=\begin{cases}\dfrac{8R\left(v_d t\right)^2 C_1}{3h}G_\infty+\dfrac{16Rv_d{}^2C_1}{3h}\displaystyle\sum_{n=1}^{N}\left\{G_nT_n\left(t+T_n\left(e^{-\frac{t}{T_n}}-1\right)\right)\right\} & if \quad t<t_{dr}\\ \dfrac{8R\left(v_d t_{dr}\right)^2 C_1}{3h}G_\infty+\dfrac{16Rv_d{}^2C_1}{3h}\displaystyle\sum_{n=1}^{N}\left\{G_nT_n e^{\frac{-(t-t_{dr})}{T_n}}\left(t_{dr}+T_n\left(e^{-\frac{t_{dr}}{T_n}}-1\right)\right)\right\} & otherwise\end{cases} \tag{21}$$

$$F_2(t)=\begin{cases}\dfrac{8\left(Rv_d t\right)^{\frac{5}{2}}C_2}{3Rh^2}G_\infty+\dfrac{10\left(Rv_d\right)^{\frac{5}{2}}C_2}{3Rh^2}\displaystyle\sum_{n=1}^{N}\left\{G_nT_n^{\frac{3}{2}}\left(\sqrt{\frac{t}{T_n}}\left(2t-3T_n\right)+3T_nD\left(\sqrt{\frac{t}{T_n}}\right)\right)\right\} & if \quad t<t_{dr}\\ \dfrac{8\left(Rv_d t_{dr}\right)^{\frac{5}{2}}C_2}{3Rh^2}G_\infty+\ldots & \\ \dfrac{10\left(Rv_d\right)^{\frac{5}{2}}C_2}{3Rh^2}\displaystyle\sum_{n=1}^{N}\left\{G_nT_n^{\frac{3}{2}}e^{-\frac{(t-t_{dr})}{T_n}}\left(\sqrt{\frac{t_{dr}}{T_n}}\left(2t_{dr}-3T_n\right)+3T_nD\left(\sqrt{\frac{t_{dr}}{T_n}}\right)\right)\right\} & otherwise\end{cases} \tag{22}$$

$$F_3(t)=\begin{cases}\dfrac{8R^2\left(v_d t\right)^3 C_3}{3h^3}G_\infty+\dfrac{8R^2v_d^3C_3}{h^3}\displaystyle\sum_{n=1}^{N}\left\{G_nT_n\left(t\left(t-2T_n\right)+2T_n{}^2\left(1-e^{\frac{-t}{T_n}}\right)\right)\right\} & if \quad t<t_{dr}\\ \dfrac{8R^2\left(v_d t_{dr}\right)^3 C_3}{3h^3}G_\infty+\dfrac{8R^2v_d^3C_3}{h^3}\displaystyle\sum_{n=1}^{N}\left\{G_nT_n e^{-\frac{(t-t_{dr})}{T_n}}\left(t_{dr}\left(t_{dr}-2T_n\right)+2T_n{}^2\left(1-e^{\frac{-t_{dr}}{T_n}}\right)\right)\right\} & ..\ otherwise\end{cases} \tag{23}$$

$$F_4(t)=\begin{cases}\dfrac{8\left(Rv_d t\right)^{\frac{7}{2}}C_4}{3Rh^4}G_\infty+\ldots & \\ \dfrac{7\left(Rv_d\right)^{\frac{7}{2}}\sqrt{t}C_4}{3Rh^4}\displaystyle\sum_{n=1}^{N}\left\{G_nT_n^3\left[\frac{t}{T_n}\left(4\frac{t}{T_n}-10\right)+15\left(1-\sqrt{\frac{T_n}{t}}D\left(\sqrt{\frac{t}{T_n}}\right)\right)\right]\right\} & if \quad t<t_{dr}\\ \dfrac{8\left(Rv_d t_{dr}\right)^{\frac{7}{2}}C_4}{3Rh^4}G_\infty+\ldots & \\ \dfrac{7\left(Rv_d\right)^{\frac{7}{2}}\sqrt{t_{dr}}C_4}{3Rh^4}\displaystyle\sum_{n=1}^{N}\left\{G_nT_n^3e^{-\frac{(t-t_{dr})}{T_n}}\left[\frac{t_{dr}}{T_n}\left(4\frac{t_{dr}}{T_n}-10\right)+15\left(1-\sqrt{\frac{T_n}{t_{dr}}}D\left(\sqrt{\frac{t_{dr}}{T_n}}\right)\right)\right]\right\} & otherwise\end{cases} \tag{24}$$

These expressions provide the complete description of the stress relaxation during the indentation of a thin soft film.

In Fig. 4, the effect of adding higher order terms on to the Hertzian model is shown. It can be seen that adding higher order terms increases the predicted force for given material properties if the film is thin. The effect decreases as the order is increased, suggesting that even higher order terms become negligible, however, it appears that those terms up to and including the second order are significant.

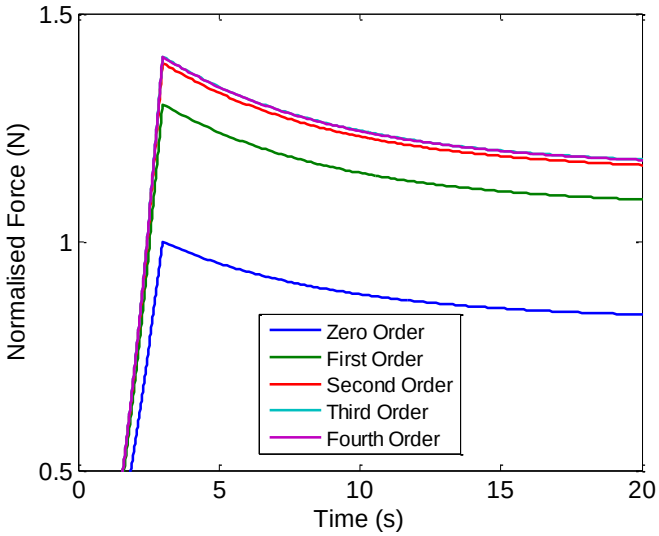

Fig. 4: Effect of adding higher order corrections to account for thin film effects. Note the uncorrected, or zero order theory, can significantly underestimate the force required to indent a thin film to a specific depth.

Experimentation

Silicone elastomer moulds were cast in 35 mm diameter poly(styrene) Petri dishes (Fisher Scientific, UK) using Sylgard mix (Type 184 Silicone Elastomer, Dow Corning, USA). The Sylgard mix consisted of the uncured elastomer and the curing agent at relative ratios of 5:1, 10:1 and 20:1 according to volume. The moulds were left to polymerise at 20 ^{o}C for a minimum of 7 days prior to use. Petri dishes were subsequently broken and removed from around the cured elastomer disk prior to performing stress relaxation measurements.

Stress relaxation measurements were performed at 18 ^{o}C and 40 % relative humidity using a Z030 mechanical tester (Zwick/Roell, UK) with a 28.5 mm diameter stainless steel sphere (Dejay Distribution, UK) attached to a 100 N load cell. The procedure for the stress relaxation measurement involved indenting the sphere a specific distance into the sample, at a velocity of 1 mm/s. This was followed by a 120 s hold period during which the indentation depth was held constant whilst the force measured by the load cell decayed. Finally, a retraction sufficiently large such that the sphere was no longer in contact with the surface was performed, also at a velocity of 1 mm/s. The surface topography of the stainless steel sphere was measured using a MicroXAM2 Interferometer (Omniscan, UK) and was found to have an average surface roughness (S_a) on the order of 25-30 nm, and therefore the sphere was considered to be continuously smooth in comparison to the indentation depth employed. The surface topography of the elastomer was measured using a NanoWizard II atomic force microscope (JPK Instruments, UK) operating in contact mode using a pyramidal-tipped Si_3N_4 cantilever (DNP-S, Veeco, UK), and was found to have an average surface roughness on the order of 2 nm.

Results and Discussion

Examples of the results of the indentation experiments can be seen in Figs. 5 and 6. By comparing Figs. 5(A) and 5(B) it is shown that the thinner samples are stiffer. This is caused by the geometric effect due to the proximity of the rigid base as discussed above.

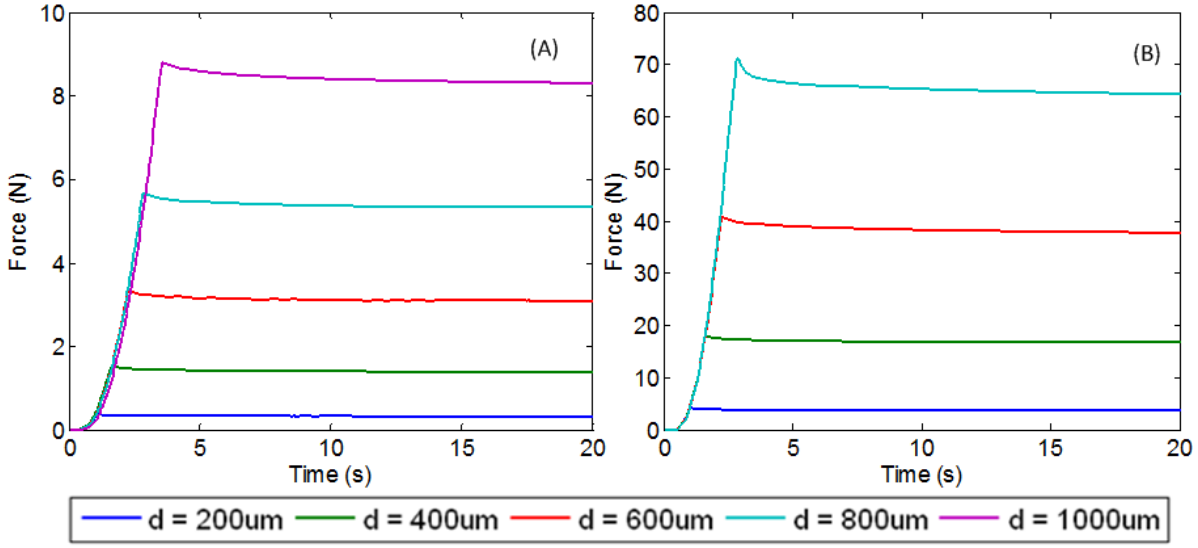

Fig. 5: Experimental stress relaxation results for the indentation of 10:1 mix PDMS for varying indentation depths. In (A) the layer thickness is 17.8 mm and in (B) 1.7 mm.

This effect is even more apparent in Fig. 6 where the same indentation experiment has been performed on the same material but with different layer thicknesses. It can be seen that the magnitude of the force is dependent on the layer thickness. In this case this is a simple geometric effect, however, in biological materials it could well be due to varying material properties. Attempting to interpret the observed behaviour using simple Hertzian theory implies that the material properties vary with depth; but when the full theory including the thickness corrections is used, the material properties are found to be constant as will be seen in Figs, 8-10.

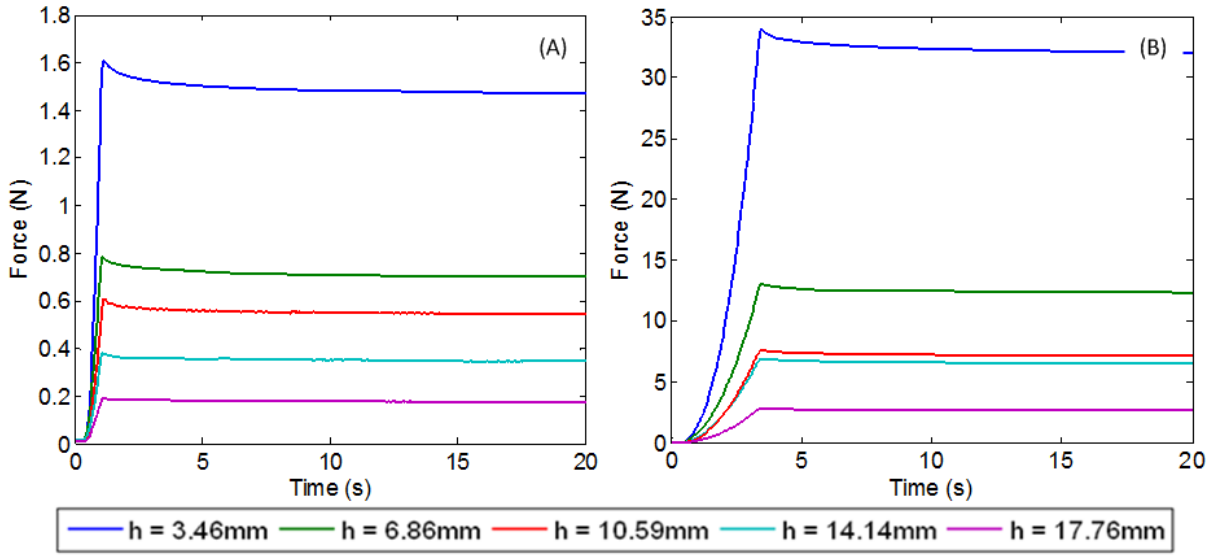

Fig. 6: Effect of layer thickness on experimental stress relaxation results for 10:1 mix PDMS at an indentation depth of (A) 200 µm and (B) 1000 µm.

The theory described above was fitted to the experimental data exemplified by Figs. 5 and 6 using a multivariate curve fitting algorithm. The algorithm was based on MatLab's (MatLab V.7.0, Mathworks, US) built-in nonlinear least-squares data-fitting function. The function which was fitted to the experimental data was formed from eqs. 9 and 23 to 26. Variables such as loading time, dwell time and maximum indentation depth were defined from the experimental set-up prior to fitting. An example of the quality of the curve fitting method is shown in Fig. 7. Two theoretical models were fitted to the experimental data, one assuming the material could be described by a single element, the other by three elements (see Appendix for details). It was assumed the material was bonded to the substrate and all corrections given by eqs. 23 to 26 were used in the fit. In the case of the single element model, it can be seen that the fit was reasonable with an R^2 value of 0.89. However, in the case of three elements being used, it can be seen that the fit exhibits greater agreement and the theory and fitted coefficients well describes the behaviour of the material. Here the fit gave a R^2 value of 0.96.

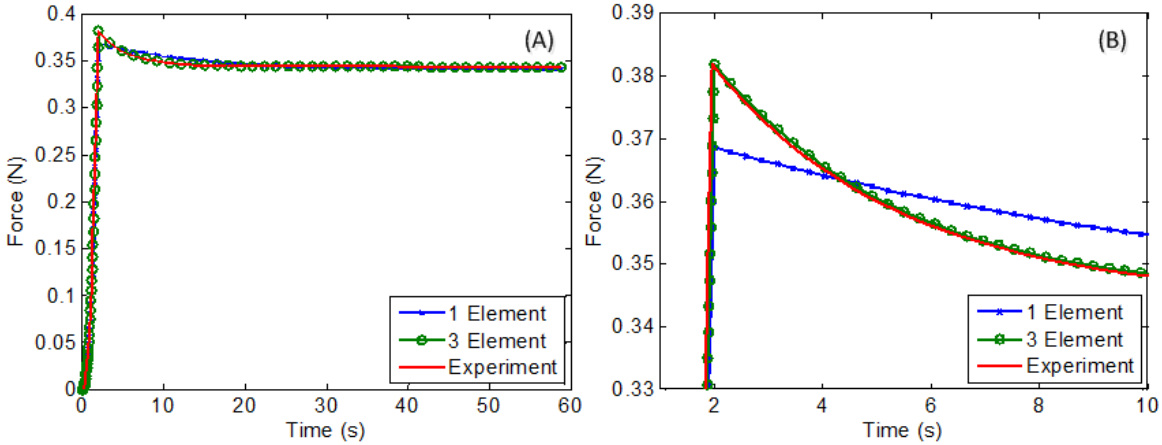

Fig. 7: Comparison between theoretical and experimental stress relaxation results for 10:1 mix PDMS with a 14.1 mm layer thickness and an indentation depth of 200 µm. All higher corrections given by eqs. 23 to 26 were used in the fitting. Two theoretical models were fitted to the data. The first assumed the material is bonded to the substrate and can be described by a single element model. The R^2 value was 0.89. The second theory assumed the material is bonded to the substrate and can be described by a three element model. The R^2 value is 0.96. In (A) the full data range is plotted and in (B) a close-up of the data in (A) is shown.

One of the most important viscoelastic properties and one of the simplest to use for comparisons of materials is the instantaneous shear modulus, G_0 as given in eq. A6. In Figs. 8 to 10, the instantaneous shear modulus has been plotted as a function of layer thickness for all penetration depths and for the three afore-mentioned theories – uncorrected (eq. 9), unbonded thin film and bonded thin film. Fig. 8 shows the calculated modulus for PDMS mixed with its curing agent at a ratio of 5:1, in Fig. 9 the ratio is 10:1 and in Fig. 10 this ratio is 20:1. It has been assumed that three elements of the standard linear model are needed to describe the material. In all three figures it can be seen that the uncorrected model predicts that the modulus increases as the layer thickness decreases. However, the corrected theories predict a more consistent value, as expected. In this instance, the theory which assumes the layer to be bonded to the substrate gives the most consistent value suggesting that the PDMS does not slip relative to the substrate surface. It is interesting to note that regardless of the indentation depth, all three theories tend to converge when the layer thickness is *c.a.* 10 to 12 mm suggesting that the additional stress due to the underlying substrate is negligible compared to the stress due to Hertzian contact at thicknesses greater than this.

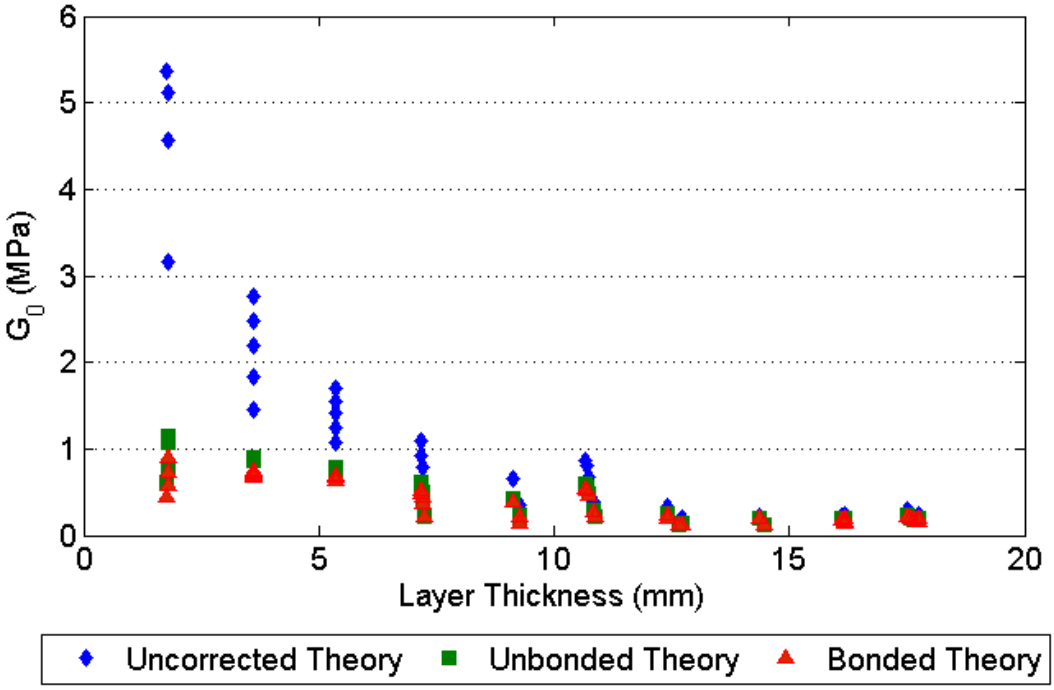

Fig. 8: Calculated instantaneous relaxation shear moduli for all penetration depths. PDMS mix ratio of 5:1. Fitted using the standard linear model with three elements.

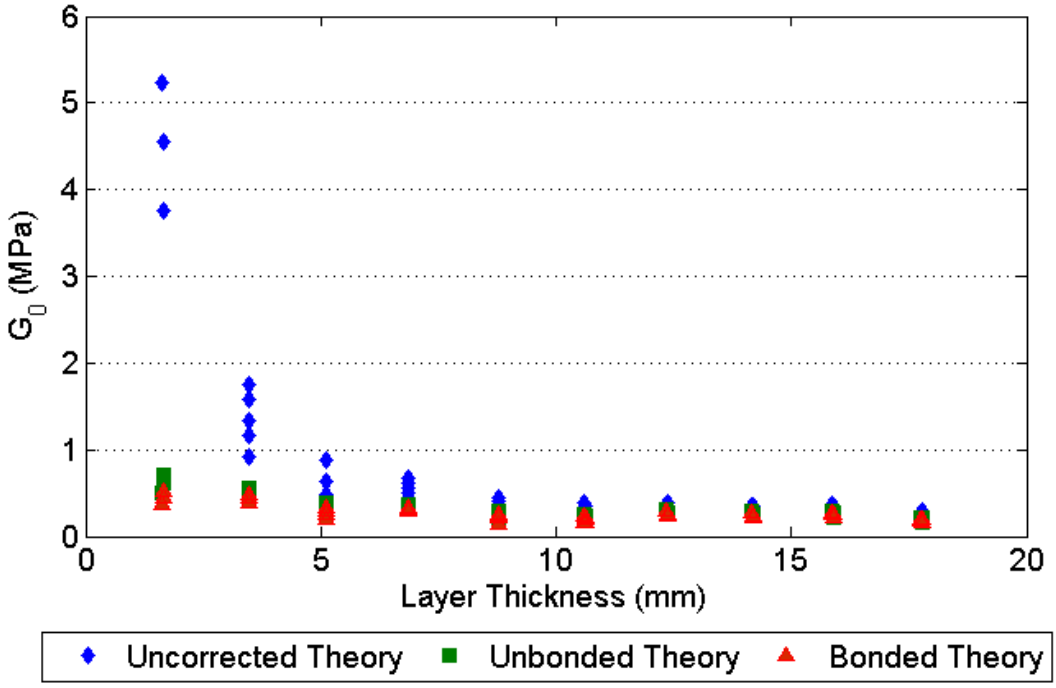

Fig. 9: Calculated instantaneous relaxation shear moduli for all penetration depths. PDMS mix ratio of 10:1. Fitted using the standard linear model with three elements.

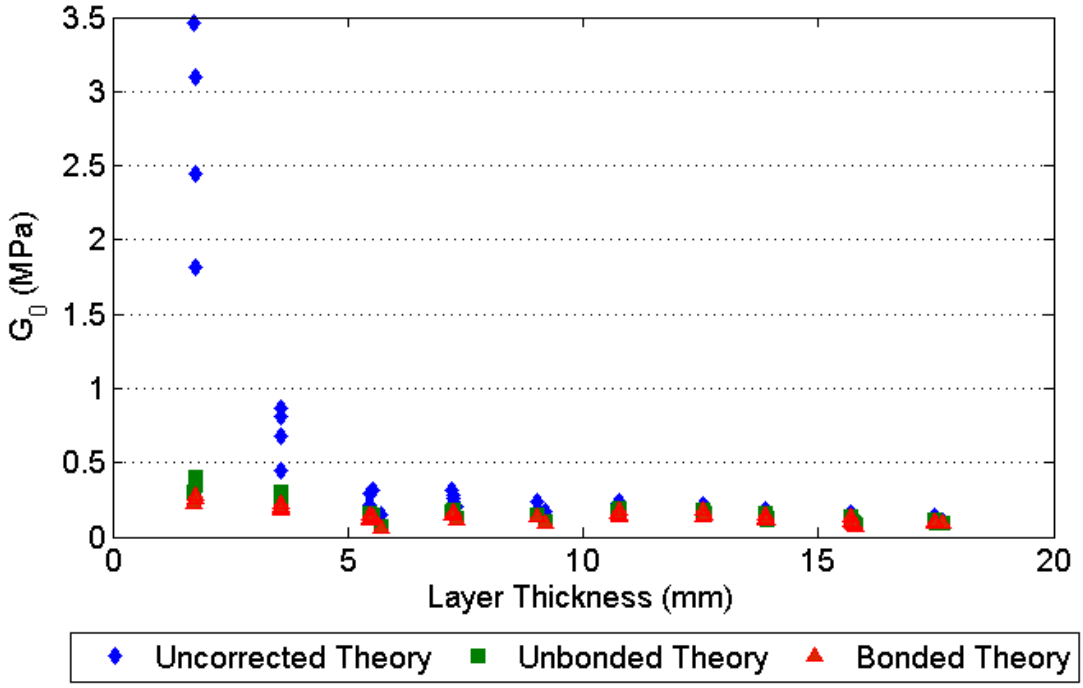

Fig. 10: Calculated instantaneous relaxation shear moduli for all penetration depths. PDMS mix ratio of 20:1. Fitted using the standard linear model with three elements.

The layer thickness also has an effect on the calculated time constants. For the case where it is assumed that a single element of the standard linear model describes the material, there is only one time constant. The time constant has been calculated from the coefficients found by fitting the three theories to the experimental data for the case where the PDMS mix ratio was 10:1 and indentation depth was 400 µm (see Fig. 14). It can be seen that the uncorrected theory predicts that the time constant is roughly the same for all layer thicknesses whereas the corrected theories predict the relaxation time should decrease as the layer thickness decreases. This prediction is consistent with the data shown in Fig. 5 and 6. In Fig. 5(A) where the layer thickness is kept constant, the relaxation time appears to be approximately equal for each run; however, in Fig. 6 the peak tends to be sharper as the layer thickness decreases, suggesting shorter relaxation times for thinner layers. Similar to the

convergence between the predicted values for the instantaneous shear modulus for the three theories, the time constants predicted by the three theories become equal to each other when the layer thicknesses is between 7 to 9 mm.

This convergence is independent of the indentation depth. In Fig. 11 the relaxation time for the same material at different indentation depths has been plotted as a function of layer thickness. The calculated time constant is consistent for each penetration depth, but again decreases as the layer thickness decreases at approximately 10 to 12 mm.

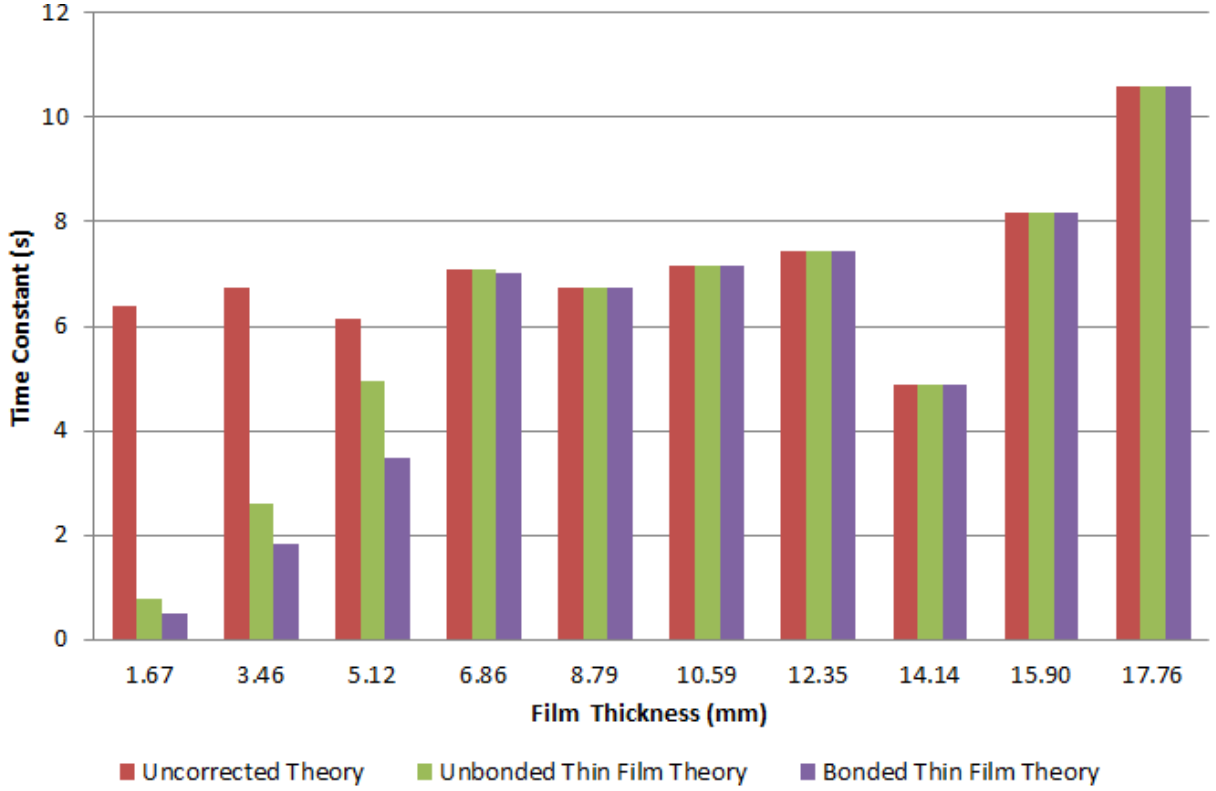

Fig. 11: Calculation of the time constants by the three theories. In all cases a single element model was assumed. Note greater correlation with increasing film thickness.

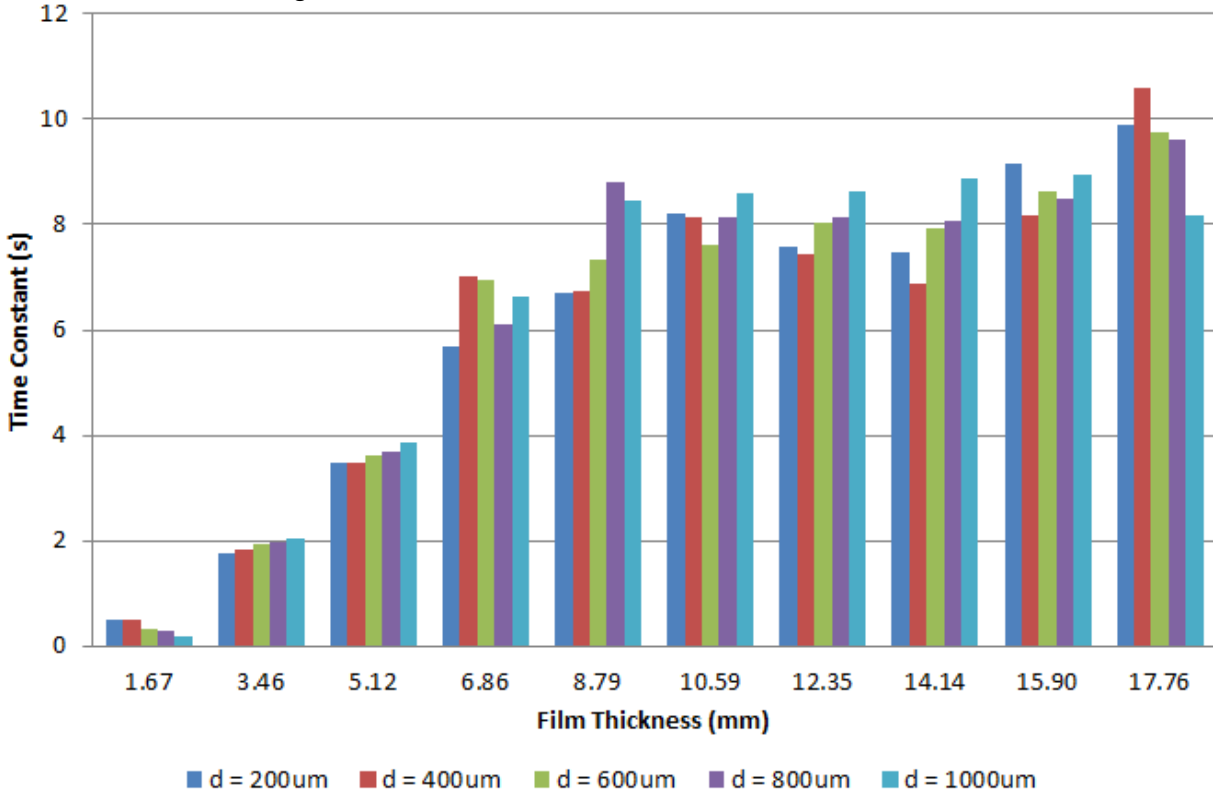

Fig. 12: Time constants as calculated using the bonded thin film theory for different penetration depths and film thicknesses. Note that the material appears to relax slower as the film gets thicker until a critical thickness when the relaxation time becomes approximately constant.

The materials tested in this work were different mixes of PDMS, a relatively tough elastomer. It was also tested using a mechanical tester and a probe 28.5 mm in diameter. This was done so that the assumptions such as the stress relaxation condition, the material being homogeneous and isotropic were all clearly met and that the theory was well suited. However, this theory is also applicable for samples which would require smaller forces and smaller displacements than required here. Hence it is possible to use this theory for analysing soft biological tissues using equipment with greater force sensitivity, such as an atomic force microscope, in a manner comparable to Darling et al. (Darling et al, 2006). Some care needs to be taken if measuring materials with multiple soft layers, as whilst effective moduli can be measured, determining the correct modulus of each layer is a non-trivial task (Cox, 2008, Pailler-Mattei et al. 2008). Similarly, if the material was nonhomogeneous, fibrous for instance, and the probe was sufficiently small as to be able to interact with the internal components of the material than it would not constitute a thin film on a rigid substrate and the higher order corrections in the theory would not be appropriate. That said if the probe used was sufficiently small compared to the fibre for instance in question then the uncorrected theory may be used.

Conclusion

The spherical indentation for a thin layer of viscoelastic material has been analysed. A model based on the work of Dimitriadis *et al.* (2002), which corrected the Hertzian model to take into account the effect of a rigid underlying substrate, has been derived which incorporates the transient nature of a stress relaxation experiment. The model assumes that the material can be described by the generalised standard linear model. The theory has been fitted to experimental data and it has been shown that the effects of the thickness of the material have been correctly taken into account. This theory can therefore be used to accurately calculate the viscoelastic properties of thin layers of soft solids.

Acknowledgments

The Z030 Mechanical Tester, MicroXAM2 Interferometer, and NanoWizard II Atomic Force Microscope used in this research were obtained, through Birmingham Science City: Innovative Uses for Advanced Materials in the Modern World (West Midlands Centre for Advanced Materials Project 2), with support from Advantage West Midlands (AWM) and part funded by the European Regional Development Fund (ERDF). This research was undertaken within the FP7-NMP NANOBIOTOUCH project (contract no. 228844). The authors are grateful for the financial support provided by the EC and the Science City Research Alliance.

Appendix

The relaxation operator has to encompass all the linear viscoelastic behaviour of the material. A classical approach to the modelling of the linear viscoelastic behaviour of real materials is based on the mechanical analogy with the response of combinations of springs and dashpots. These models are useful for representing materials whose relaxation does not occur at a single time but in a set of times, perhaps due to being made of molecular segments of different lengths or affected by different relaxation processes. A constitutive model that can predict a distribution of both creep and stress relaxation phenomena and so give a realistic representation of viscoelastic solid materials is the generalised standard linear solid model (Ferry 1980). This model consists of N single elements in parallel whereby each element is comprised of a spring in series with a Kelvin-Voigt element as shown in Fig. A1:

Fig. A1: A schematic of the generalised standard linear solid model comprised of *N* single elements connected in parallel.

The stress-strain relationship for each element is given by:

$$\eta_n k_{1n} \dot{\gamma} + k_{1n} k_{2n} \gamma = \left(k_{1n} + k_{2n}\right)\sigma + \eta_n \dot{\sigma} \qquad n = 1 \ldots N \tag{A1}$$

The strain is the same for each element, therefore the total stress acting on the system is:

$$\sigma = \sum_{n=1}^{N} \sigma_n \tag{A2}$$

The stress can therefore be solved for the case of a step change in strain, γ_0, to give:

$$\sigma(t) = \Psi(t)\gamma_0 = \sum_{n=1}^{N}\left[\left(\frac{k_{1n}k_{2n}}{k_{1n}+k_{2n}}\right)+\left(\frac{{k_{1n}}^2}{k_{1n}+k_{2n}}\right)e^{-t/T_n}\right]\gamma_0 \quad \text{(A3)}$$

where $T_n = \eta_n/(k_{1n}+k_{2n})$ are the relaxation time constants. Therefore, the relaxation operator for the material can be written as a Prony series:

$$\Psi(t) = \sum_{n=1}^{N}\left[\left(\frac{k_{1n}k_{2n}}{k_{1n}+k_{2n}}\right)+\left(\frac{{k_{1n}}^2}{k_{1n}+k_{2n}}\right)e^{-t/T_n}\right] \quad \text{(A4)}$$

The shear relaxation modulus defined as $G(t) = \sigma(t)/(2\gamma_0)$ (Oyen, 2006) for a material described by eq. A4 is:

$$G(t) = \frac{1}{2}\sum_{n=1}^{N}\left[\left(\frac{k_{1n}k_{2n}}{k_{1n}+k_{2n}}\right)+\left(\frac{{k_{1n}}^2}{k_{1n}+k_{2n}}\right)e^{-t/T_n}\right] \quad \text{(A5)}$$

There are two important limits to eq. A5. Namely when $t=0$, $G(0)$ describes the instantaneous shear modulus of the material, i.e. the shear modulus experienced during an impulsively applied strain, and is given by:

$$G_0 = G(0) = \sum_{n=1}^{N}\frac{k_{1n}}{2} \quad \text{(A6)}$$

The other limit is when $t=\infty$. In this case $G(\infty)$ gives the relaxed shear modulus i.e. the steady state modulus experienced when a strain has been held constant for sufficient time that the stress is also constant. $G(\infty)$ is given by:

$$G_\infty = G(\infty) = \frac{1}{2}\sum_{n=1}^{N}\left(\frac{k_{1n}k_{2n}}{k_{1n}+k_{2n}}\right) \quad \text{(A7)}$$

Using this nomenclature and using G_n to indicate the coefficients to the exponential functions in eq. A5, eq. A4 is simplified to:

$$\Psi(t) = 2G_\infty + 2\sum_{n=1}^{N}G_n e^{-t/T_n} \quad \text{(A8)}$$

In the text when a three element model is being used to fit to the data it is being assumed that a shear modulus given by eq. A5 when $N=3$, as given in full in eq. A9, describes the mechanical behaviour of the material.

$$\begin{aligned} G(t) = {} & \frac{1}{2}\left[\left(\frac{k_{11}k_{21}}{k_{11}+k_{21}}\right)+\left(\frac{k_{12}k_{22}}{k_{12}+k_{22}}\right)+\left(\frac{k_{13}k_{23}}{k_{13}+k_{23}}\right)\right] \\ & + \frac{1}{2}\left(\frac{{k_{11}}^2}{k_{11}+k_{21}}\right)e^{-t/T_1} + \frac{1}{2}\left(\frac{{k_{12}}^2}{k_{12}+k_{22}}\right)e^{-t/T_2} + \frac{1}{2}\left(\frac{{k_{13}}^2}{k_{13}+k_{23}}\right)e^{-t/T_3} \end{aligned} \quad \text{(A9)}$$

References

Bufler H (1971) Theory of elasticity of a multilayered medium. J. Elast., 1:125-143

Cao Y, Ma D, Raabe, D (2009) The use of flat punch indentation to determine the viscoelastic properties in the time and frequency domains of a soft layer bonded to a rigid substrate, Acta Biomater., 5(1): 240-248

Chadwick RS (2002) Axisymmetric indentation of a thin incompressible layer. SIAM J. App. Math., 62(5):1520-1530

Chen WT (1971) Computation of stresses and displacements in a layered elastic medium. Int. J. Eng. Sci., 9:775–800

Chen WT, Engel PA (1972) Impact and contact stress analysis in multilayer media. Int. J. Solids Struct, 8:1257-1281

Cox MAJ, Driessen NJB, Boerboom RA, Bouten CVC, Baaijens FPT (2008) Mechanical characterization of anisotropic planar biological soft tissues using finite indentation: Experimental feasibility. J. Biomat. 41:422-429

Darling EM, Zaucher S, Guilak F (2006) Viscoelastic properties of zonal articular chondrocytes measured by atomic force microscopy. Osteo. Arth. Cart., 14:571-579

Darling E M., et al. (2007) Thin-layer model for viscoelastic, stress-relaxation testing of cells using atomic force microscopy: do cell properties reflect metastatic potential? Biophys. J., 92:1784-1791

Dhaliwal RS, Rau IS (1970) The axisymmetric Boussinesq problem for a thick elastic layer under a punch of arbitrary profile. Int. J. Engr. Sci., 8:843-856
Dimitriadis EK et al., (2002) Determination of elastic moduli of thin layers of soft material using the atomic force microscope. Biophys. J., 82:2798-2810
Dintwa E, Tijskens E, Ramon H (2008) On the accuracy of the Hertz model to describe the normal contact of soft elastic spheres, Granular Matter 10:209-221
Domke J, Radmacher M (1998) Measuring the elastic properties of thin polymer films with the atomic force microscope. Langmuir, 14:3320-3325
Ferry JD (1980) Viscoelastic properties of polymers. 3rd Ed., Wiley, New York
Fretigny C, Chateauminois A (2000), Solution for the elastic field in a layered medium under axisymmetric contact loading. J. Phys. D: Appl. Phys., 40:5418-5428
Graham GAC, Sabin GCW (1973) The correspondence principle of linear viscoelasticity for problems that involve time-dependent regions, Int. J. Eng. Sci., 11(1):123-140
Greenwood JA (2010) Contact between an axisymmetric indenter and a viscoelastic half-space. Int. J. of Mech. Sci., 52(6):829-835
Hertz H (1882) Uber die Beruhrung fester, elastischer Korper. J. Reine Angew. Math., 92:156-171
Jardet V, Morel P (2003) Viscoelastic effects on the scratch resistance of polymers: relationship between mechanical properties and scratch properties at various temperatures. Progress in Organic Coatings, 48(2-4):322-331
Johnson KL (1985) Contact mechanics. CUP, Cambridge
Landau LD, Liftshitz EM (1986), Course of theoretical physics: Theory of elasticity. Elsevier
Lee EH, Radok JRM (1960) The contact problem for viscoelastic bodies. J. App. Mech. Trans. ASME, 27:438-444
Levental I, et al. (2010) A simple indentation device for measuring micrometer-scale tissue stiffness. J. Phys.: Condens. Matter, 22:194120
Moreno-Flores S, et al. (2010) Stress relaxation and creep on living cells with the atomic force microscope: a means to calculate elastic moduli and viscosities of cell components. Nanotech., 21:445101
Oyen ML (2006) Analytical techniques for indentation of viscoelastic materials. Philos. Mag. 86: 33, 5625-5641
Pailler-Mattei C, Bec S, Zahouani H (2008) In vivo measurements of the elastic mechanical properties of human skin by indentation tests. Med. Eng. Phys. 30:599-606
Rizzo FJ, Shippy DJ (1971) An application of the correspondence principle of linear viscoelasticity theory. 21(2):321-336
Ting TCT (1966) The contact stresses between a rigid indenter and a viscoelastic half-space. J. App.Mech. Trans. ASME, 27:845-854
Tu Y-O, Gazis DC (1964) The contact problem of a plate pressed between two spheres. Trans. ASME J. Appl. Mech., 31:659-666
Wakatsuki T, et al. (2001) Effects of cytochalasin D and latrunculin B on mechanical properties of cells. J. Cell Sci., 114(5):1025-1036
Zhang CY, Zhang YW, Zeng KY (2004) Extracting the mechanical properties of a viscoelastic polymeric film on a hard elastic substrate. J. Mater. Res. 19(10):3053-3061